Journal of Solid State Chemistry 182 (2009) 749–756

Contents lists available at ScienceDirect

Journal of Solid State Chemistry

journal homepage: www.elsevier.com/locate/jssc

Morphological and phase evolution of TiO_2 nanocrystals prepared from peroxotitanate complex aqueous solution: Influence of acetic acid

Jeong Ah Chang, Muga Vithal, In Chan Baek, Sang Il Seok *

KRICT-EPFL Global Research Laboratory, Advanced Materials Division, Korea Research Institute of Chemical Technology, 19 Sinseongno, Yuseong, Daejeon 305-600, Republic of Korea

ARTICLE INFO

Article history:
Received 15 October 2008
Received in revised form
20 December 2008
Accepted 30 December 2008
Available online 6 January 2009

Keywords:
TiO_2 nanocrystals
Morphological control
Peroxotitanate complex
Chemical modification
Effects of acetic acid

ABSTRACT

Nanosized anatase and rutile TiO_2 having different shape, *phase* and size have been prepared from aqueous solutions of peroxo titanium complex starting from titanium(IV) isopropoxide (TTIP), acetic acid and hydrogen peroxide (H_2O_2) in water/isopropanol media by a facile sol–gel process. The TiO_2 nanocrystals are characterized by powder X-ray diffraction (XRD), Raman spectroscopy, FT-IR spectroscopy, TEM, high resolution transmission electron microscopy (HRTEM) and selected area electron diffraction (SAED) techniques. The influence of pH and the sequence of addition of reaction contents on the phase and morphology of TiO_2 are studied. The reasons for the observation of only anatase and/or mixture of anatase and rutile are given.

1. Introduction

Nanosized titania (TiO_2) is currently attracting academic and industrial community due to its unique combination of properties. A few of these properties are good scattering effect, high dielectric constant and refractive index, ability to exhibit different electrical characteristics, chemical and biological inertness, strong oxidizing power, and long term stability against corrosion [1,2]. Further, titania is water stable, non-toxic, less expensive and environmentally benign. Such an amalgamation of properties have culminated its use as white pigment paint, optical coating/beam splitter, solar energy converter, photocatalyst, humidity and oxygen sensor and environmental devices [3–5]. For most of these applications, the crystalline form (anatase or rutile), size, and morphology of titania are critically important with reference to its performance. For instance, the enhancement of solar energy conversion efficiency in dye sensitized solar cells is dependent on the size, *phase* and morphology of TiO_2. Similarly, the photo degradation of salicylic acid by TiO_2 aero gel (porosity 90%, surface area 600 $m^2 g^{-1}$) was about 10 times to that of commercially available Degussa TiO_2 [6]. Thus, in the preparation of nanotitania, its phase and morphology control play prominent roles in titania based devices.

Several preparative methods of nanotitania are reported. A majority of them belong to wet chemical route, the advantages of which are well documented [7,8]. The prominent wet chemical methods are sol–gel [8–13] and hydrothermal [11–17]. Sol–gel method is one of the simplest, cost effective, versatile and most commonly used methods of obtaining nanosized titania. Nanosized TiO_2 with different morphologies such as particles, rods, tubes, wires, sheets, mesoporous and aerogels are prepared by sol–gel method [18–21]. Various parameters such as pH, presence/absence of catalyst, temperature, chelating reagent and the nature of precursor influence the *size*, *shape* and *phase* of target material considerably in the sol–gel process. Sugimoto et al. [10,11] have studied the influence of (a) pH on the size control and (b) various amines on the shape control of anatase nanoparticles prepared from sol–gel process using TTIP. Chemseddine and Moritz [8] have examined the control over the crystal structure, size, shape and organization of TiO_2 nanocrystals using $Ti(OR)_4$ and tetra methyl ammonium hydroxide (Me_4NOH) by wet chemical route and accounted for the growth mechanism and super lattice formation. A comprehensive review on the chemical modification of titanium alkoxides by various organic donors and the hydrolysis behavior of resultant organically modified precursor was reported by Schubert [22,23]. Attar et al. [12] have reported the effect of modifier ligands (acetic acid and acetyl acetone) on the nanotitania formation from TTIP by sol–gel method. Rozes et al. [24] have reviewed the studies made on the titanium-oxo clusters and their derivatives.

Compared to hydrothermal method of preparing nanotitania, the wet chemical route using peroxo titanium complex is less explored [25–27]. Although the system, TTIP–CH_3COOH, is investigated earlier [12,22,23,28–30], to the best of our knowledge the evolution of titania from this system in the presence of H_2O_2 is not reported so far. In this paper we report the effect of pH on the phase and morphology evolution of nanotitania from

* Corresponding author. Fax: +82 42 8614151.
E-mail addresses: seoksi@krict.re.kr, seoksi@pado.krict.re.kr (S.I. Seok).

0022-4596/$ - see front matter © 2009 Elsevier Inc. All rights reserved.
doi:10.1016/j.jssc.2008.12.024

peroxo titanium complex in the presence of acetic acid as chelating agent.

2. Experimental section

Titanium(IV) tetraisopropoxide [$Ti(OCH(CH_3)_2)_4$ or TTIP, Aldrich, 97%], hydrogen peroxide (H_2O_2, Aldrich, 35 wt% aqueous solution), acetic acid (CH_3COOH, or AcOH, Aldrich, 99.8%) and isopropyl alcohol [$(CH_3)_2CHOH$ or IPA, Aldrich, 99.7%] were used as received without any further purification.

Fig. 1 shows schematically the three synthetic routes (methods A, B and C) used for preparing TiO_2 nanocrystals. Method A was part of our earlier investigation [26]. In the present investigation, two methods (B and C) were adopted to synthesize TiO_2 nanocrystals.

Method A: A solution of TTIP (20 mmol) in 10 ml of IPA was added drop wise into 100 ml of solution containing 1 mol of H_2O_2 under constant stirring in a round bottom flask. (Note that an exothermic reaction occurs after 20–30 min. The vessel should be sufficiently cooled to prevent the overflow of reaction contents). The resultant orange titanium complex solution was refluxed for 12–24 h in a controlled temperature oil bath preheated to 100 °C. The refluxed product was dried at 60 °C to obtain pale yellow TiO_2 powder and designated as a1 (H_2O_2/TTIP). (Note that the chemicals given in the parenthesis indicate the sequence of their addition. The chemical present at the right side is added to the chemical present at left side. Flower bracket is to be executed first, if present.) In another experiment, a solution of TTIP (20 mmol) in 10 ml of IPA was added drop wise into a round bottom flask containing 100 ml of distilled water. The resultant sol was centrifuged and thoroughly washed with water to eliminate IPA. The TiO_2 sol is dried at 60 °C to yield the product TiO_2 a2 (water/TTIP).

Method B: In a round bottom flask, 100 ml of solution containing 1 mol of H_2O_2 (pH = 3.4–3.5) was taken (step 1). To this solution, 20 mmol of TTIP in 10 ml of IPA was added drop wise with constant stirring. A light orange titanium peroxo complex solution was obtained (step 2) (pH = 1.1–1.2). Glacial acetic acid (60 mmol) was added drop wise under vigorous stirring to titanium peroxo complex solution and the resultant sol (pH = 1.1–1.2) was aged at 100 °C (24 h) followed by *drying* at 60 °C. The resultant TiO_2 was designated as b1 [(H_2O_2/TTIP)/AcOH]. In another experiment, 20 mmol of TTIP in 10 ml of IPA was added drop wise to the solution containing glacial acetic acid (60 mmol, 3.4 ml) in a round bottom flask (pH = 3.9–4.1). To the resultant solution, 100 ml of water is added. The solution thus obtained (pH = 3.3–3.4) was aged at 100 °C (24 h) followed by *drying* at 60 °C. The obtained TiO_2 was named as b2 [(AcOH/TTIP)/water].

Method C: In this method, 20 mmol of TTIP in 10 ml of IPA was taken in a round bottom flask (step 1). Glacial acetic acid (60 mmol) was added drop wise to the stirred TTIP producing pale yellow solution (step 2) (pH = 3.9–4.1). It is believed that $Ti(O^iPr)_{4-x}(OAc)_x$ is formed at this stage [31]. This resultant solution was added drop wise into 100 ml of solution containing 1 mol of H_2O_2 under constant stirring (step 3) in a round bottom flask. The pH of solution decreased to 1.1. Thus obtained orange sol as peroxotitanate complex was aged at 100 °C (24 h) followed by *drying* at 60 °C. The resulting TiO_2 was named as c1 [H_2O_2/(TTIP/AcOH)]. In a different experiment, the pale yellow solution obtained in step 2, was added into 100 ml of water. The resultant solution (pH = 3.3–3.4) was aged at 100 °C (24 h) followed by *drying* at 60 °C to yield product c2 [water/(TTIP/AcOH)]. (Note that in experiments leading to products b2 and c2 the order of addition was reversed.)

The X-ray diffraction (XRD) patterns obtained on an X-ray diffractometer (Rigaku, D/Max II) using Cu$K\alpha$ radiation ($\lambda = 0.1542$ nm) were used to characterize the crystalline phase and size of TiO_2 nanocrystals. The phase content of anatase ($2\theta = 25.3$ of (101) line, JCPDF no: 21-1272) and rutile ($2\theta = 27.4$ of (110) line, JCPDF no: 21-1276) were estimated using the equation given in the literature [32]. The average crystalline size (D) is estimated using Scherrer equation in the spherical shape [33]. The Raman spectra were recorded with Raman spectrometer (Bruker, Equinox 55) using a Nd:YAG laser. The morphology and size characteristics of TiO_2 nanocrystals were measured by transmission electron microscope (TEM) (FEI, Tecnai G2) operating at 200 kV. The high-resolution transmission electron microscopy (HRTEM) images and selected area electron diffraction

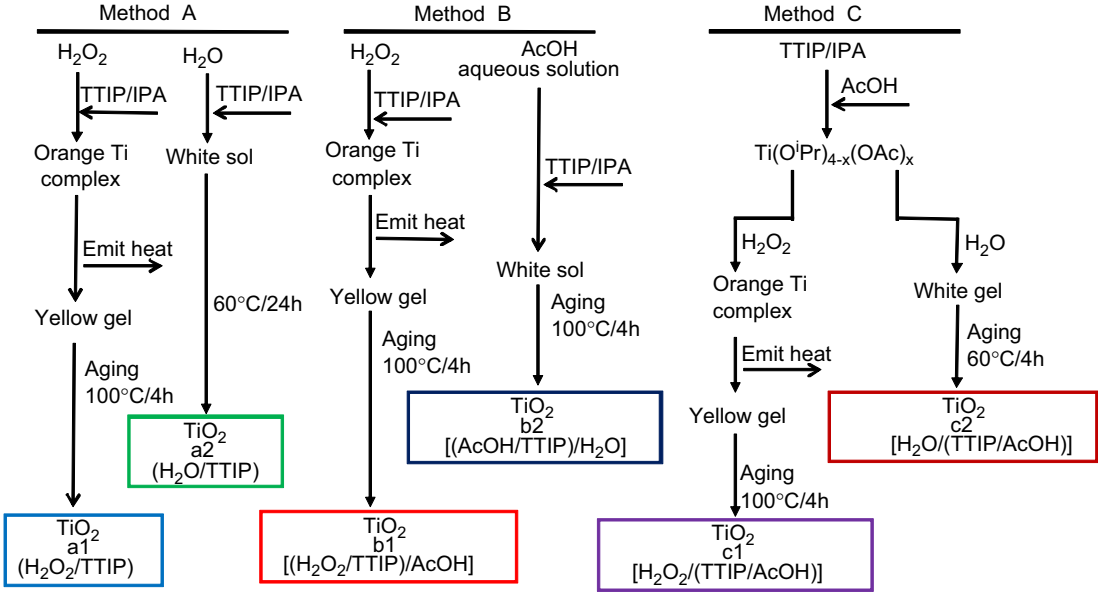

Fig. 1. Flow chart for preparation of different TiO_2 nanocrystals via sol–gel process (100 °C, 24 h) by methods A, B, and C: the reaction of unmodified Ti precursor as titanium isopropoxide [$Ti(O^iPr)_4$] and modified Ti precursor by acetic acid (AcOH) in the presence of H_2O_2 (TiO_2 as #a1, #b1, #c1) and absence of H_2O_2 (TiO_2 as #a2, #b2, #c2) aqueous solution is shown.

(SAED) images were recorded using a JEOL TEM-2010F. FT-IR (Bio-Rad Win-IR, FTS-165 spectrometer) was used to characterize the presence of acetic acid on the surface of the TiO_2 nanocrystals.

3. Results

3.1. XRD and Raman studies

The powder XRD of b1 [(H_2O_2/TTIP)/AcOH] was found to be crystalline and characterized by diffraction peaks belonging to both anatase and rutile (Fig. 2, left). The relative percentage of anatase and rutile calculated using equation given in the literature [32] was 57% and 43%, respectively. The diffraction lines were relatively broad indicating the nanosize of crystallites. The particle size of anatase and rutile calculated using Scherer's formula [33] was 14 and 12 nm, respectively. The powder XRD of b2 [(AcOH/TTIP)/water] shows diffraction lines corresponding to anatase without any trace of other TiO_2 phases. The particle size of anatase (b2) calculated using Scherer's formula [33] was 6 nm. The broad base line observed in powder XRD of b1 and b2 indicates the presence of small quantity of amorphous phase. The Raman spectrum of sample b1 (Fig. 2, right) shows the bands at 149 (strong), 397 (weak), 445 (weak), 515 (weak) and 634 cm^{-1}

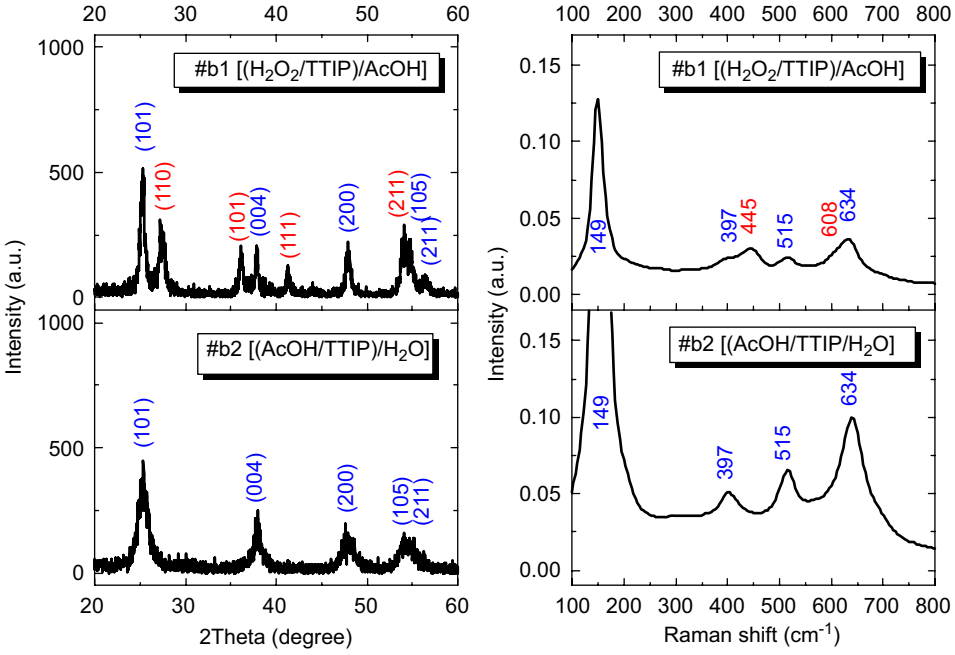

Fig. 2. Powder XRD patterns (left) and Raman spectra (right) of TiO_2 nanocrystals synthesized by sol–gel method (100 °C, 24 h, by method B).

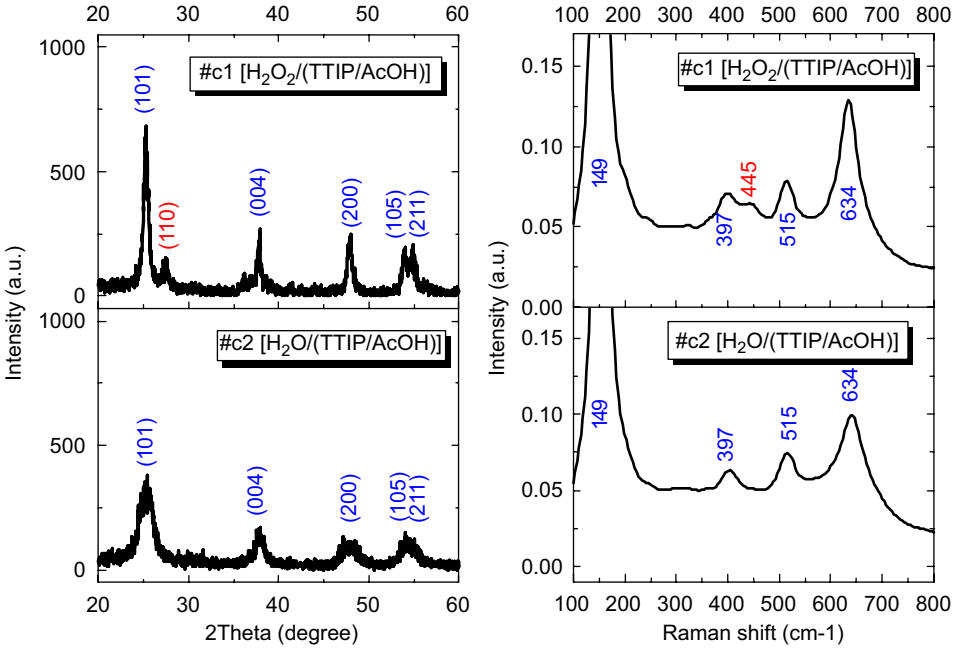

Fig. 3. Powder XRD patterns (left) and Raman spectra (right) of TiO_2 nanocrystals prepared by sol–gel method (100 °C, 24 h, by method C).

(medium, shoulder like). The bands observed at 149, 397, 515 and 634 cm^{-1} are consistent with the bands observed for anatase TiO_2 while the band observed at 445 cm^{-1} belongs to rutile TiO_2 [34,35]. The other Raman bands expected for crystalline rutile (143, 612 cm^{-1}) are submerged in the Raman bands of anatase phase [34,35]. The Raman spectrum of b2 is consistent with anatase phase. Thus the Raman spectral results are in accordance with powder XRD observations. The powder XRD of c1 [H_2O_2/(TTIP/AcOH)] shows peaks belonging to anatase (92%) and rutile (8%) while that of c2 [water/(TTIP/AcOH)] exhibits only anatase (Fig. 3, left). The Raman spectra of c1 and c2 are consistent with its XRD results (Fig. 3, right).

3.2. TEM and HRTEM studies

Further structural characterization of the TiO_2 samples was carried out using TEM image analysis. Fig. 4 shows the TEM images of a1, a2, b1, b2, c1, and c2. The TEM images of a2, b2, and c2 show aggregated spherical TiO_2 nanocrystallites of size ~5 nm.

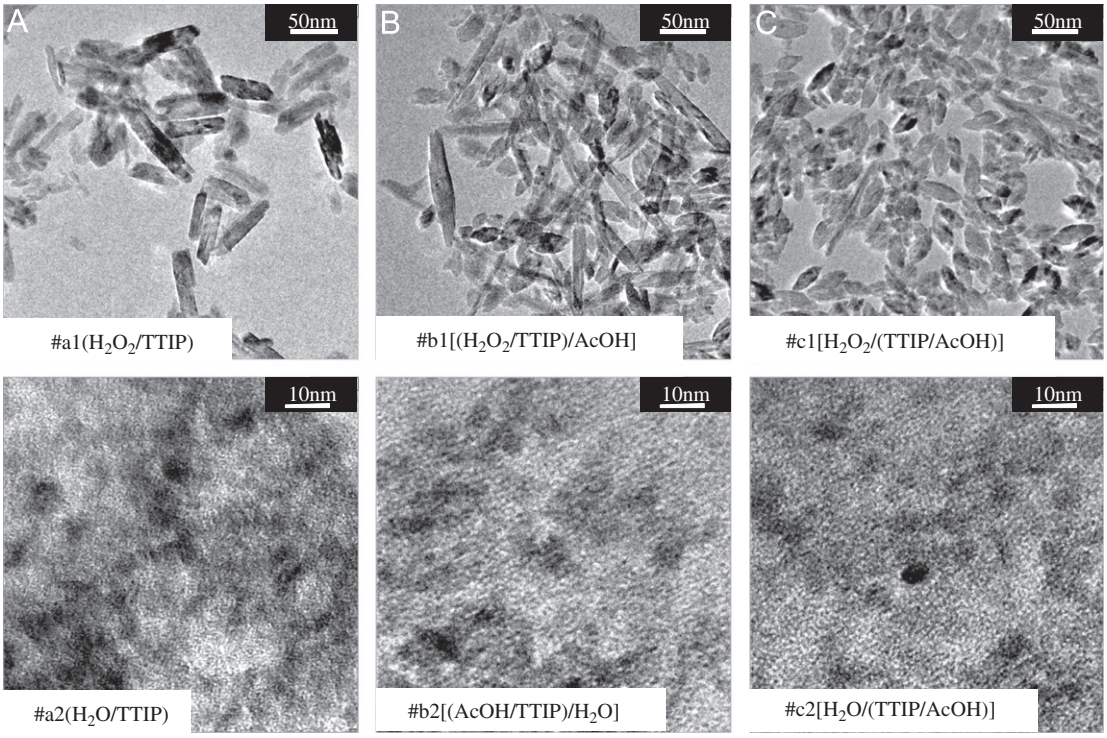

Fig. 4. TEM images of different TiO_2 nanocrystals synthesized by methods A, B and C in the presence of H_2O_2 aqueous solution (#a1, #b1, #c1) and the absence of H_2O_2 aqueous solution (#a2, #b2, #c2).

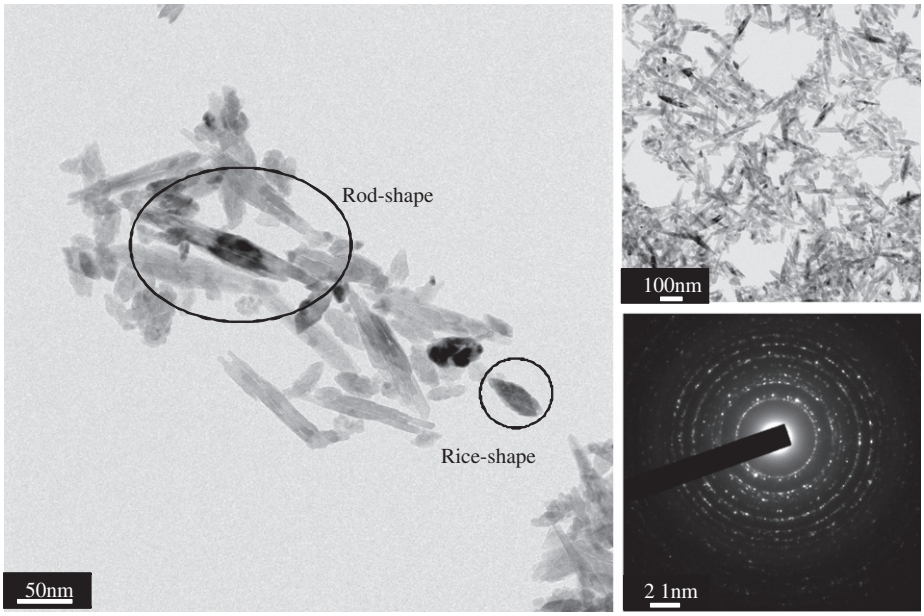

Fig. 5. TEM images and SAED (ring pattern) of TiO_2 nanocrystals of #b1.

Fig. 5 shows the TEM image of b1 sample. It consists of "rice like" anatase (15×30 nm) and "rod like" (ellipsoidal) rutile (20×100 nm) (shown in circles in Fig. 5). The electron diffraction image clearly indicates highly crystalline nature of the sample. The "rod shape" rutile exhibits substantial polydispersity in terms of its length and width compared to "rice shape" anatase. The HRTEM image of "rice shape" anatase of sample b1 is shown in Fig. 6. This nanocrystal is viewed along (101) plane and elongated in the (001) direction. The lattice fringes shown in the HRTEM image corresponding to distances 3.4 and 4.84 Å agree well with distances of (101) and (002) lattice planes, respectively, of anatase TiO_2 [36]. The selected area diffraction pattern (SAED) shown in Fig. 6 also confirm the single crystalline anatase phase. The lateral width of "rice shape" anatase obtained from TEM result is about 15 nm which also agrees with the number of (101) lattice planes. The HRTEM image of "rod shape" rutile of sample b1 is shown in Fig. 7. This TiO_2 nanocrystal is grown in the (001) direction. The width of this nanocrystal, estimated from the number of (110) planes present is 26 nm. The lattice fringes shown in the HRTEM image corresponding to distances 3.0 and 3.36 Å agree well with distances of (001) and (110) lattice planes, respectively, of rutile TiO_2 [37]. The SAED shown in Fig. 7 also confirm the single crystalline rutile phase.

3.3. FT-IR studies

In Fig. 8, the FT-IR spectrum of b1 [$(H_2O_2$/TTIP)/AcOH] shows bands at 1629, 1517, 1430, and 1384 cm^{-1}. The band observed at 1629 cm^{-1} are due to O–H stretching and deformation mode of H_2O, respectively, while the bands at 1517 and 1430 cm^{-1} belong to asymmetric v_{as} and symmetric v_s of carboxyl (COO) group, and

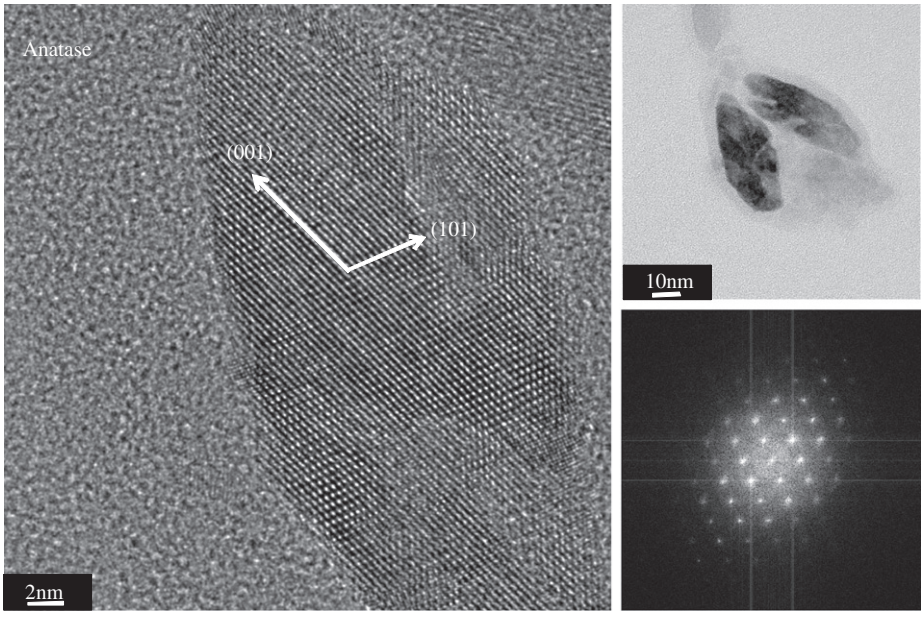

Fig. 6. HRTEM images and SAED (spot pattern) of anatase TiO_2 nanocrystals in rice shape (samples b1 and c1).

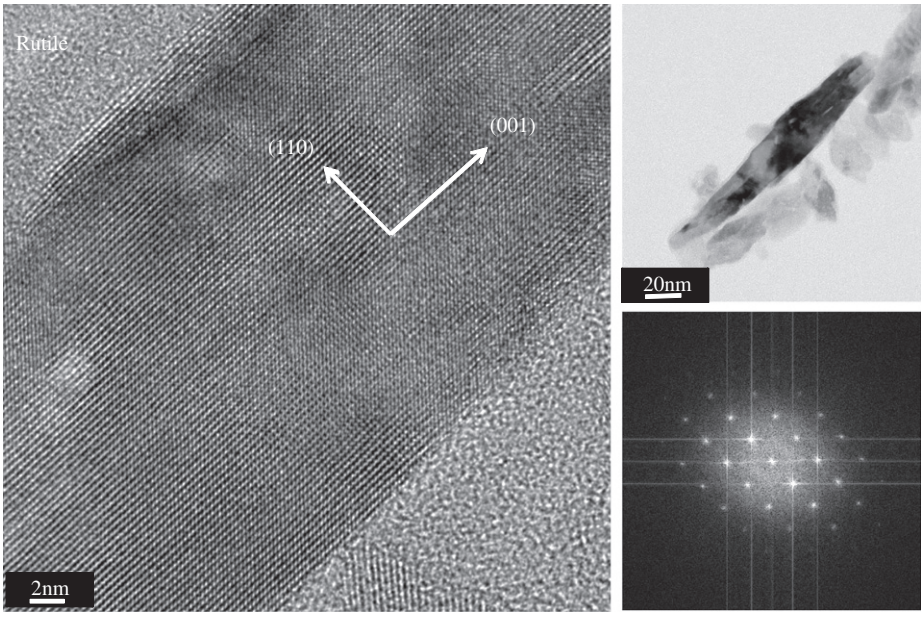

Fig. 7. HRTEM images and SAED (spot pattern) of rutile TiO_2 nanocrystal in rod shape (sample b1).

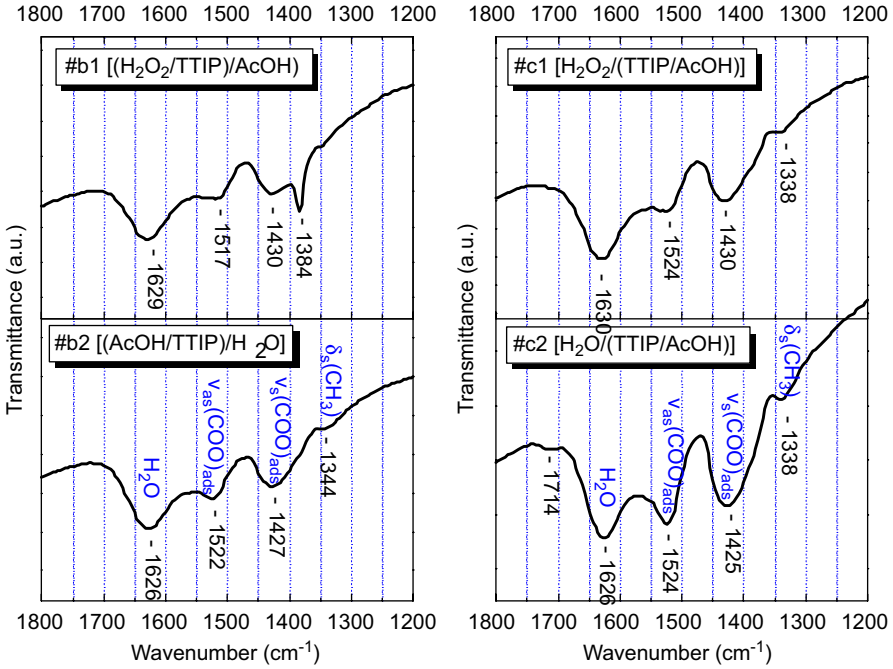

Fig. 8. FT-IR spectra of TiO_2 nanocrystals synthesized by sol–gel method (100 °C, 24 h, by methods B, C).

the weak band at 1384 cm^{-1} is attributed to $\delta(CH_3)$ of acetate adsorbed on to the surface of titania [38]. The magnitude of wave number difference, $\Delta\nu_{obs} = \nu_{as}(COO) - \nu_s(COO)$, observed in transition metal carboxylates compared to $\Delta\nu$ in the free state (i.e. $\Delta\nu_{ionic}$), gives information regarding the binding mode of carboxylate groups on metal oxide surfaces [39]. In most of the transition metal carboxylates, it was observed that for monodentate mode of binding, $\Delta\nu_{obs} > \Delta\nu_{ionic}$ while for bridge type, $\Delta\nu_{obs} < \Delta\nu_{ionic}$. Similar behavior is expected for acetate adsorbed onto TiO_2. For acetic acid, $\Delta\nu_{ionic}$ is found to be 137 cm^{-1} [38]. In the present investigation, $\Delta\nu_{obs} = 87\ cm^{-1}$ for b1 sample indicating the "bridge" mode of binding to the TiO_2 surface. The magnitude of $\Delta\nu$ for b2, c1 and c2 samples was found to be of the same order. These values are close to those reported earlier for acetate adsorbed onto TiO_2 nanoparticles [40]. The infrared spectra of b2, c1 and c2 are similar to that of b1 except for the small variations in the positions.

4. Discussion

The powder XRD, Raman, and TEM results of b1 [(H_2O_2/TTIP)/AcOH], b2 [(AcOH/TTIP)/water], c1 [H_2O_2/(TTIP/AcOH)] and c2 [water/(TTIP/AcOH)] indicate that the presence of chelating reagent and/or ligands (AcOH and H_2O_2) and their sequence of addition influence the phase formation and morphology of TiO_2 considerably. First consider the cases of TiO_2 products b2 and c2 which are prepared in the absence of H_2O_2. Both these samples crystallize in anatase phase. Addition of TTIP to AcOH or vice versa forms the complex $Ti(^iOPr)_{4-x}(OAc)_x$ which hydrolyses to a composition which is approximately represented as $Ti(OH)_{4-x}(OAc)_x$. It is well known that acetate ligand decreases the rate of hydrolysis and results in the formation of smaller particles [33]. Further, addition of AcOH to TTIP or vice versa gives a solution whose pH is in the range 3.9–4.1 which is favorable for anatase formation [16,41]. In the present investigation, the morphology of b2 and c2 products is spherical with size of ~5 nm. Why anatase is preferentially formed in b2 and c2 products? The explanation is given later.

Now consider the cases of b1 [(H_2O_2/TTIP)/AcOH] and c1 [H_2O_2/(TTIP/AcOH)] which were prepared in the presence of H_2O_2. In both these samples, a mixture of anatase and rutile was obtained with preponderance of anatase in c1. In considering the preparation of b1, the pH of H_2O_2 solution used was in the range 3.4–3.5. The drop wise addition of TTIP into this solution gives peroxo titanium complex whose pH is 3.4–3.5 at the beginning of addition but decreases considerably. The peroxo complex hydrolyses and the pH is favorable for anatase nucleation. As the addition of TTIP continues, the pH decreases to 1.1 and the nucleation of rutile begins. Thus, the rate of nucleation process for rutile and anatase formation will be approximately same yielding rutile and anatase of approximately same quantity. Addition of acetic acid after the addition of TTIP into H_2O_2 solution has little effect as the peroxo titanium complex has been already hydrolyzed and the nucleation of both anatase and rutile started. Addition of TTIP to hydrogen peroxide solution results in the formation of peroxo complex whose structure (monomeric or dimeric) is dependent on the pH of the solution. The possible reaction is

$$\begin{aligned} &Ti(^iO\,Pr)_4 + H_2O_2 + 3H_2O \\ &\quad \rightarrow [Ti(OH)_3(OOH)] + 4^i\,Pr\,OH \\ &\quad \rightarrow [O = Ti(OH)(OO)]^- + H^+ + H_2O \end{aligned} \tag{1}$$

The decrease in pH value is due to the liberation of protons during the formation of peroxo complex.

Now consider the preparation of sample c1 (H_2O_2/{TTIP/AcOH}). Addition of acetic acid to TTIP (in IPA) results in the formation of complex $Ti(O^iPr)_{4-x}(OAc)_x$. The pH of [(TTIP/AcOH)] was in the range 3.9–4.1. Upon the addition of this solution containing $Ti(O^iPr)_{4-x}(OAc)_x$ into H_2O_2 solution leads to peroxo complex of $Ti(O^iPr)_{4-x}(OAc)_x$ which hydrolyses slowly due to the presence of acetate group and the nucleation of anatase begins. The pH of the resultant solution decreased very slowly. At the end of addition of $Ti(O^iPr)_{4-x}(OAc)_x$ into H_2O_2 solution, the pH decreased to 1.5 and the nucleation of rutile begins. Thus, the rate of nucleation of rutile lags far behind the rate nucleation of anatase giving rise to predominantly anatase phase in the product c1.

The mechanism of formation of different forms of titania by hydrothermal methods has been addressed by several groups [8,17,24,42–46]. It is observed that the mechanism of titania formation (from hydrothermal or sol–gel) is related to the structure of the polymorphs of TiO_2. In all the three phases of titania, the basic unit is octahedral TiO_6. The rutile phase is characterized by linear chains of TiO_6 octahedra that share a pair of opposite edges while in anatase each TiO_6 octahedron shares four edges with different octahedra forming zigzag chains. In brookite phase, three edges of TiO_6 octahedron are shared by other octahedral [47]. Yanagisawa and Ovenstone [17] proposed the mechanism of anatase and rutile nucleation from their detailed investigation of crystallization of amorphous TiO_2 in neutral, acidic and basic conditions by hydrothermal method. They have concluded that: (i) water has catalytic effect on the crystallization of amorphous TiO_2, (ii) presence of acid favors rutile and brookite formation and (iii) chloride ion accelerates the nucleation of anatase. Yin et al. [42] have formulated the mechanism for the anatase and rutile formation via face sharing and edge sharing of TiO_6, respectively, and explained the chelating effect of citric acid in the rutile formation. Li et al. [43] have investigated the synthesis of high photoactive nanotitania powders from aqueous $TiOCl_2$ solutions and proposed the mechanism for the formation of anatase and rutile by dehydration of surface OH groups catalyzed by H^+ or H_3O^+. Chemseddine and Moritz [8] have explained the formation of anatase nanocrystals, clusters, rods, slabs and polymers by the condensation of TiO_6 octahedra by olation pathway making use of partial charge model proposed by Henry et al. [45].

The evolution of titania and the influence of pH on the phase formation from sol–gel process in the presence of hydrogen peroxide have received less attention. Zhang et al. [41] have investigated the effect of pH on titania formation by sol–gel process from experimental and theoretical (DFT/B3LYP) approaches. They have observed that: (a) nanocrystalline rod like rutile was formed from pH 2 precursor solution, (b) granular anatase was formed from pH 4 and 9 precursor solutions, and (c) granular anatase and rutile resulted from pH 7 precursor solution. It was noticed that the pH of the solution critically decides the composition of hydrolyzed product which in turn determines the type of titania phase [16,41]. In the present investigation, both b2 and c2 products are characterized by only anatase. The pH of (AcOH/TTIP) or (TTIP/AcOH) solutions (i.e. the solution of $[Ti(O^iPr)_{4-x}(OAc)_x]$ was in the range 3.9–4.1. Addition of this solution into water or vice versa gave a solution whose pH was in the range 3.2–3.5. Hydrolysis of $[Ti(O^iPr)_{4-x}(OAc)_x]$ in this pH range is favorable for anatase nucleation. Thus, both b2 and c2 are expected to yield only anatase. During the preparation of b1, drop wise addition of TTIP into H_2O_2 solution drops the pH from 3.4–3.5 to 1.1 in short span of time leading to the nucleation of both anatase and rutile in almost equal proportions. In the preparation of c1, drop wise addition of (TTIP/AcOH) or $Ti(O^iPr)_{4-x}(OAc)_x$ into H_2O_2 solution, the pH drops from 3.9–4.1 to 1.5 rather slowly leading to predominantly anatase (92%) with trace of rutile. The "rice" shaped morphology of anatase in c1 has a diameter of $\approx$15 nm but its length varies in the range 20–50 nm indicating substantial polydispersity. The morphology of anatase observed in the present work is similar to that observed by Chemseddine and Moritz in their work of condensation of $Ti(OR)_4$ in the presence of Me_4NOH [8]. The nucleation of anatase starts with dimerization of $Ti(OH)_x$ units which are connected by one vertex to form the basic unit. The dimeric units are the basic building blocks for the crystallization of all polymorphs of titania. In accordance with the partial charge model, these dimers condense to form skewed chains as result of olation and oxolation processes leading to growth of anatase crystal along (001) plane resulting "rice like" morphology [44,45].

It is worth comparing the present results with our earlier reported (samples a1 and a2) observations [26]. Addition of TTIP into aqueous H_2O_2 solution (sample a1) gives peroxo titanium complex which hydrolyses to form $Ti(OH)_x$ or $TiO_2.xH_2O$. The peroxo group facilitates the formation of rutile TiO_2 nanorods depending on the ratio of (TTIP/H_2O_2) [29,30]. In the present investigation, it was observed that addition of AcOH to TTIP followed by H_2O_2 (sample c1) leads to predominantly (92%) anatase while the addition of TTIP to H_2O_2 followed by AcOH (sample b1) gives approximately equal quantities of anatase and rutile. Thus it appears that the sequence of addition plays crucial role in the titania phase evolution by an eventual change of pH in the solution via the formation of different titanium precursors.

5. Conclusion

Phase pure spherical anatase of size ~5 nm was obtained from the system TTIP/AcOH irrespective of sequence of addition. In the presence of H_2O_2, the relative percentage of "rice shape" anatase and "rod shape" rutile depends on the sequence of addition of AcOH and H_2O_2. The dimensions of "rice shape" anatase and "rod shape" are about 15×30 nm (width $\times$ length) and 15×30 nm–20×100 nm (width $\times$ length), respectively, and the growth is along (001) direction. The FT-IR spectra of all the samples show the adsorption of acetic acid on to the TiO_2 nanoparticles via "bridge" mode of coordination. TEM and HRTEM results show highly crystalline nature of samples. The explanation for observation of only anatase and/or anatase and rutile mixture was given.

Acknowledgments

This research was supported both by the Korea Foundation for International Cooperation of Science & Technology through the Global Research Lab. (GRL) Program funded by the Ministry of Education, Science and Technology, by a Grant from the Fundamental R&D Program for Core Technology of Materials funded by the Ministry of Knowledge Economy, and Republic of Korea. One of the authors (M. Vithal) is thankful to the Korean Federation of Science and Technology Society (KOFST) for inviting him as visiting scientist under Brain Pool Program.

Appendix A. Supplementary material

Supplementary data associated with this article can be found in the online version at doi:10.1016/j.jssc.2008.12.024.

References

[1] X. Chen, S.S. Mao, Chem. Rev. 107 (2007) 2891.
[2] H.D. Nam, B.H. Lee, S.-J. Kim, C.-H. Jung, J.-H. Lee, S. Park, Jpn. J. Appl. Phys. 37 (1998) 4603.
[3] B.O. Regan, M. Graetzel, Nature 353 (1991) 737.
[4] A. Fujishima, K. Honda, Nature 238 (1972) 37.
[5] M.R. Hoffmann, S.T. Martin, W. Choi, D.W. Bahnemann, Chem. Rev. 95 (1995) 69.
[6] G. Dagan, M. Tomkiewich, J. Phys. Chem. 97 (1993) 12651.
[7] A. Chemsiddine, H. Jungblut, S. Boulmaaz, J. Phys. Chem. 100 (1996) 12546.
[8] A. Chemseddine, A. Moritz, Eur. J. Inorg. Chem. (1999) 235.
[9] T. Moritz, J. Reiss, K. Diesner, D. Su, A. Chemsiddine, J. Phys. Chem. B 101 (1997) 8052.
[10] T. Sugimoto, X. Zhou, A. Muramastu, J. Colloid Interface Sci. 259 (2003) 43.
[11] T. Sugimoto, X. Zhou, A. Muramastu, J. Colloid Interface Sci. 259 (2003) 53.

[12] A.S. Attar, M.S. Ghamsari, F. Hajesmaeilbaigi, S. Mirdamadi, J. Mater. Sci. 43 (2008) 1723.
[13] P.D. Cozzoli, A. Kornowski, H. Weller, J. Am. Chem. Soc. 125 (2003) 14539.
[14] S.Y. Chae, M.K. Park, S.K. Lee, T.Y. Kim, S.K. Kim, W.I. Lee, Chem. Mater. 15 (2003) 3326.
[15] Q. Zhang, L. Gao, Langmuir 19 (2003) 967.
[16] H. Yin, Y. Wada, T. Kitamura, S. Kambe, S. Murasawa, H. Mori, T. Sakata, S. Yanagida, J. Mater. Chem. 11 (2001) 1694.
[17] K. Yanagisawa, J. Ovenstone, J. Phys. Chem. 103 (1999) 7781.
[18] C.J. Barbe, F. Arendse, P. Comte, M. Jirousek, F. Lenzmann, V. Shklover, M. Gratzel, J. Am. Ceram. Soc. 80 (1997) 3157.
[19] M.D. Wei, Y. Konishi, H. Zhou, H. Sugihara, H. Arakawa, J. Electrochem. Soc. 153 (2006) A1232.
[20] Z. Miao, D.S. Xu, J.H. Ouyang, G.L. Guo, X.S. Zhao, Y. Tang, Nano Lett. 2 (2002) 717.
[21] L. Crepaldi, G.J.d.A.A. Soler-Illia, D. Grosso, F. Cagnol, F. Ribot, C. Sanchez, J. Am. Chem. Soc. 125 (2003) 9770.
[22] U. Schubert, J. Mater. Chem. 15 (2005) 3701.
[23] M.-A. Neouze, U. Schubert, Monatsh. Chem. 139 (2008) 183.
[24] L. Rozes, N. Stenou, G. Fornasiera, C. Sanchez, Monatsh. Chem. 137 (2006) 501.
[25] S.I. Seok, B.Y. Ahn, N.C. Pramanik, H. Kim, J. Am. Ceram. Soc. 89 (2006) 1147.
[26] J.A. Chang, M. Vithal, I.C. Baek, S.I. Seok, J. Nanosci. Nanotechno., in press.
[27] Y. Gao, H. Luo, S. Mizusugi, M. Nagai, Cryst. Growth Des. 8 (2008) 1804.
[28] R. Parra, M.S. Goes, M.S. Castro, E. Longo, P.R. Bueno, J.A. Varela, Chem. Mater. 20 (2008) 143.
[29] N. Stenou, F. Robert, K. Boubekeur, F. Ribot, C. Sanchez, Inorg. Chim. Acta 279 (1998) 144.
[30] D.P.J. Birnie III, J. Mater. Sci. 35 (2000) 367.
[31] N.R. Neale, A.J. Frank, J. Mater. Chem. 17 (2007) 3216.
[32] H. Zhang, J.F. Banfield, J. Phys. Chem. B 104 (2000) 3481.
[33] J. Yu, L. Zhang, B. Cheng, Y. Su, J. Phys. Chem. C 111 (2007) 10582.
[34] P.P. Lottici, D. Bersani, M. Braghini, A. Montenero, J. Mater. Sci. 28 (1993) 177.
[35] U. Balachandran, N.G. Eror, J. Solid State Chem. 42 (1982) 276.
[36] TiO_2 (anatase), JCPDF card no. 21-1272.
[37] TiO_2 (rutile), JCPDF card no. 21-1276.
[38] F.P. Rotzinger, J.M. Kesselman-Truttmann, S.J. Hug, V. Shklover, M. Gratzel, J. Phys. Chem. B 108 (2004) 5004.
[39] G.B. Deacon, F. Huber, J. Phillips, Inorg. Chem. Acta 41 (1985) 104.
[40] L. Ojamae, C. Aulin, H. Pedersen, P.-O. Kall, J. Colloid Interface Sci. 296 (2006) 71.
[41] W. Zhang, S. Chen, S. Yu, Y. Yin, J. Cryst. Growth 308 (2007) 122.
[42] H. Yin, Y. Wada, T. Kitamura, S. Kambe, S. Murasawa, H. Mori, T. Sakata, S. Yanagida, J. Mater. Chem. 11 (2001) 1694.
[43] Y. Li, N.-H. Lee, D.-S. Hwang, J.S. Song, E.G. Lee, S.-J. Kim, Langmuir 20 (2004) 10838.
[44] J. Livage, M. Henry, C. Sanchez, Prog. Solid State Chem. 18 (1988) 259.
[45] M. Henry, J.P. Jolivet, J. Livage, Struct. Bond. 77 (1992) 155.
[46] D.C. Bradley, Adv. Chem. 23 (1959) 10.
[47] V.W.H. Bauer, Acta Crystallogr. 14 (1961) 214.